Nuclear Magnetic Resonance Line Shape from Strained Gaussian Networks

M. Warner,* P. T. Callaghan,† and E. T. Samulski‡

Cavendish Laboratory, Madingley Road, Cambridge CB3 0HE, U.K.

Received December 9, 1996; Revised Manuscript Received May 28, 1997[⊗]

ABSTRACT: Elastomers when strained become anisotropic, as seen by birefringence and NMR line splitting. Brereton has shown that the fundamental model of high polymers, the ideal Gaussian chain, does not yield a split but merely a broadened line on straining. This underpinning analytic result directs one to consider richer models for chains in elastomers. We correct an error in Brereton's Gaussian analysis. The nonsplit result is retained, but the lines show some qualitative changes in shape from the results he presented. We use a method similar to his but taylored to future calculations for NMR of nematic and paranematic networks with rigid rods. We present an analytic formula for the second moment of the line shape as a function of extension λ.

I. Introduction

In an important paper, Brereton[1] addressed three aspects of the orientational localization of links in elastomers. He presented (i) an exact analytical method for deriving the NMR line shape one would observe in isotropic and strained classical elastomers and thereby showed (ii) that the NMR line of deuterons in the monomers of the chain strands of the network is broadened but unsplit, even when the network is anisotropic because of the imposed strain. This counterintuitive result is at variance with experiment and demands (iii) that to adequately model elastomers one must go beyond classical Gaussian chains even at melt densities. He introduced steric interactions and obtained a line splitting on the imposition of strain. At the end of this paper we mention other options to obtain a splitting.

Here we correct a minor error in his analytical lineshape formula. This correction does not change his qualitative point (ii) that ideal Gaussian lines remain unsplit irrespective of strain. It is useful to have a correct, analytical expression for the NMR of the fundamental model of networks. Moreover, certain qualitative features of the line shape do change on correction, and we illustrate this in plots. Additionally, we present an analytical formula for the second moment of the line shape with changing extension. Although we shall find that on extension or compression intensity is moved out from the center of the line, the second moment is not minimal in the relaxed state but at a slight compression. Thus, although we find lines for deformed elastomers must cross the line for the undeformed elastomer, the crossings are subtle for small deformations. The second moment of lines is newly accessible to high accuracy by experiment. Having an analytical expression makes obvious considerable qualitative deviations (of unexpected sign) from the predictions from Gaussian chains. We discuss new theory and experiment in section III.C.

We shall rederive the master formula in a manner parallel to Brereton but in polar rather than cylindrical coordinates. This is partly because these methods, once developed, can be used to address problems in rather richer systems, such as nematic networks with rodlike cross-links.[2−5] Orientational localization drastically effects mechanical properties if rigid-rod cross-links are employed and if the cross-linking is at least two-stage, preferably with the second stage carried out in the nematic state. These effects include moduli that depend on the strain and order during cross-linking,[2] the variation of the threshold to a nematic striped state induced by strain applied perpendicular to the director,[3,5] residual nematic order (birefringence) in unstrained elastomers at high temperatures,[2,5] and, as a related corollary, supercritical behavior in the thermal transitions of nematic elastomers that apparently remember via their rod-links the fields applied during their genesis.[2] The complex mechanical and nematic properties of these systems can be modeled by considering the behavior of the links.[6] NMR will be a powerful tool to understand these mechanical phenomena; prediction of line shape will be addressed elsewhere using the methods of this paper.

II. Orientation in Gaussian Networks

Consider a freely-jointed chain of N links of length b, the jth link's direction being specified by a unit vector $\mathbf{u}_j$. For a fixed end-to-end vector $\mathbf{R} \equiv b\sum_{j=1}^{N}\mathbf{u}_j$, the free energy (and hence the probability of finding the link in a given state) of the jth link depends on its position $\mathbf{x}_j$ and orientation $\mathbf{u}_j$; the sections of chain connecting its ends to $\mathbf{R}$ and $\mathbf{O}$ will fluctuate and act as entropic springs, their stored energy depending on how they are stretched by the choice of $\mathbf{x}_j$ and orientation $\mathbf{u}_j$ (see Figure 1). We show in a brief appendix that allowing the link j to fluctuate over all positions $\mathbf{x}_j$ with the strand end-to-end vector fixed at $\mathbf{R}$ gives an orientational potential $p(\mathbf{u}_j\cdot\mathbf{R})$ acting on the link. It is thereby oriented about $\mathbf{R}$ and has a uniaxial order parameter tensor $\check{\mathbf{Q}} = Q(R)\,(^3/_2\hat{\mathbf{R}}\hat{\mathbf{R}} - {}^1/_2\check{\delta})$, where $\check{\delta}$ is the unit tensor. In this frame the magnitude of the order is $Q(R)$. $\hat{\mathbf{R}}$ is the unit vector defining the direction of $\mathbf{R} = R\hat{\mathbf{R}}$. Q is small and depends on the magnitude R of the strand but not on the link number j:

$$Q(R) = \frac{3}{5}\left[\frac{R}{(N-1)b}\right]^2 \qquad (1)$$

On average $Q \sim 1/N$. Treating the links as rods, rather

* Author to whom correspondence is addressed.

† Present address: Department of Physics, Massey University, Palmerston North, New Zealand.

‡ Present address: Department of Chemistry, University of North Carolina at Chapel Hill, Chapel Hill, North Carolina 27599-3290.

[⊗] Abstract published in *Advance ACS Abstracts,* July 15, 1997.

S0024-9297(96)01803-7 CCC: $14.00

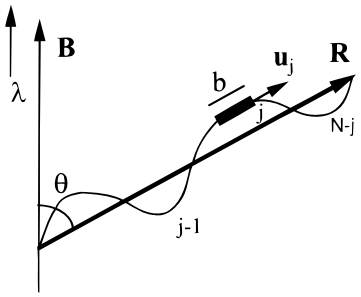

Figure 1. Given strand with end to end vector **R** of the network showing the link j of length b with a direction $\mathbf{u}_j$. The remaining links are represented as random walk chains of lengths $j - 1$ and $N - j$ appended to each end of the link j. The stretch direction is also that of the NMR field **B**. The strand vector forms an angle θ with **B**.

than as extensible Gaussian bonds,[7] has its utility when considering highly oriented nematic elastomers and when modeling[6] the Finkelmann paranematic elastomers with rigid rods we mentioned above.

III. NMR Line Structure

Consider a single nucleus (typically a deuteron) on a link belonging to a strand with fixed end-to-end vector **R**. The interaction of the quadrupole with the local electric field gradient in the motional narrowing limit causes line shifts $\Delta\omega_{\mathbf{R}}$ associated with the orientational localization of the links of this strand:

$$\Delta\omega_{\mathbf{R}} = \pm\omega_0\left(\frac{R}{R_0}\right)^2 P_2(\cos\theta) \tag{2}$$

where ω_0 is the natural frequency of interaction, $R_0^2 = Nb^2$ is the mean-square dimension of the chains and $3/5N$ has been absorbed into ω_0. The strand span **R** forms an angle θ with the NMR magnetic field. We shall adopt a reduced frequency $x = \Delta\omega/\omega_0$ and set $\cos\theta = y$. In these variables the doublet of lines is $D(x) = \sum_{\pm}\delta(x \pm z^2P_2(y))$ (with total weight $\int \mathrm{d}x\, D(x) = 2$), where $z = R/R_0$ is a reduced span size. By concentrating on nuclear quadrupole resonance, we ensure that effects are due to monomer self-correlations. Considering the interaction of proton pairs as in conventional NMR investigations of orientational order, there is a possibility of protons not on the same monomer interacting, thereby clouding the interpretation of the line splitting.

A. Isotropic Networks. The angles y are uniformly distributed and the chain magnitudes R are distributed according to $R^2\exp[-3R^2/2R_0^2]$. Counting the splittings due to orientational localization of links from all strands, one has a line shape $W(x) \equiv g_+(x) + g_-(x)$:

$$W(x) = \sum_{\pm}\frac{\int_0^\infty \mathrm{d}z\, z^2\int_{-1}^1 \mathrm{d}y\, \exp[-3z^2/2]\delta(x \pm z^2P_2(y))}{2\int_0^\infty \mathrm{d}z\, z^2\exp[-3z^2/2]} \tag{3}$$

In g_+ one performs $\int \mathrm{d}y\ \delta(x - z^2/2 + {}^3/_2z^2y^2) = \int \mathrm{d}y\ \delta(b(y - y_0)(y + y_0))$ with $y_0 = \sqrt{(z^2/2 - x)/(3z^2/2)}$ and $b = 3z^2/2$. There are contributions of $1/(2by_0)$ from strands with angles $y = \pm y_0$. This angle must be real; thus, strands must be large enough that $z > \sqrt{2x}$ and $\int \mathrm{d}z$ is accordingly restricted. Similar manipulations with g_- yield overall

$$W(x) = \frac{\sqrt{2/3}}{2\int_0^\infty \mathrm{d}z z^2\exp[-3z^2/2]} \times \left[\int_{\sqrt{2x}}^\infty \mathrm{d}z\, \frac{z}{\sqrt{z^2/2 - x}}\exp[-3z^2/2] + \int_{\sqrt{x}}^\infty \mathrm{d}z\, \frac{z}{\sqrt{z^2/2 + x}}\exp[-3z^2/2]\right] \tag{4}$$

By substitutions $z^2/2 - x = q^2/3$ and $z^2/2 + x = q^2/3$, respectively, one obtains

$$W(x) = 2\sqrt{3}[2\cosh(3x) - \exp[3x]\,\mathrm{erf}[\sqrt{9x/2}]] \tag{5}$$

B. Strained Networks. For a strained elastomer, we assume an affine deformation of strand spans, $\mathbf{R}' = \check{\lambda}\mathbf{R}$ where $\mathbf{R}'$ is the strand vector after a uniaxial deformation $\check{\lambda}$ is applied to the system: $\check{\lambda} = \check{\delta}/\sqrt{\lambda} + (\lambda - 1/\sqrt{\lambda})\mathbf{nn}$. The elastomer is extended by a factor λ along a direction **n** and shrinks by a factor of $1/\sqrt{\lambda}$ in the perpendicular directions. The new span is characterized by the new separation R' and new angle $y' = \cos\theta'$:

$$R'^2 = R^2\left[\frac{1}{\lambda} + \left(\lambda^2 - \frac{1}{\lambda}\right)y^2\right] \tag{6}$$

$$y'^2 = \lambda^2y^2/\left[\frac{1}{\lambda} + \left(\lambda^2 - \frac{1}{\lambda}\right)y^2\right] \tag{7}$$

One proceeds exactly as before, still using R and y as variables since these are appropriate to the original state of the elastomer where the probabilities of obtaining spans were set. Thus, the $g_\pm$ factors are given by $g_\pm \sim \delta(x \pm (R'/R_0)^2P_2(y'))$, which simplifies when eqs 6 and 7 are used. The line shape is

$$W_\lambda(x) = \frac{1}{2\int_0^\infty \mathrm{d}z\, z^2\exp[-3z^2/2]} \times \sum_{\pm}\int_0^\infty \mathrm{d}z\, z^2\int_{-1}^1 \mathrm{d}y\, \exp[-3z^2/2] \times \delta\left(x \mp \frac{1}{2}\frac{z^2}{\lambda} \pm \frac{1}{2}\left(2\lambda^2 + \frac{1}{\lambda}\right)z^2y^2\right) \tag{8}$$

Now the constraints are $z > \sqrt{2\lambda z}$ in g_+ and $z > \sqrt{x/\lambda^2}$ in g_-. Collecting terms, we obtain

$$W_\lambda(x) = \frac{6}{\sqrt{2\lambda + 1/\lambda^2}}[2\cosh(3\lambda x) - \exp[3\lambda x]\,\mathrm{erf}(\sqrt{[3(2\lambda + 1/\lambda^2)x/2]})] \tag{9}$$

This corrects the principal ideal Gaussian result of Brereton[1] (eq 3.8). Our x and his Ω reduced frequencies are related by $x = \Omega/2$. The argument of his erfc should be $\sqrt{3\Omega(2\lambda+1/\lambda^2)/2}$. Also, in our line shape $W(x)$ we have chosen a normalization such that the total weight of a line remains 2 as λ changes (Brereton normalizes by the zero-frequency value of the $\lambda = 1$ line: $W_1(0)$ in our notation). We thereby illustrate (a) how intensity is shifted to higher x as the network is strained—to be expected since alignment is greater and hence the splitting in any given link is greater, thus contributing to a wider line—and (b) that lines of greater λ must cross

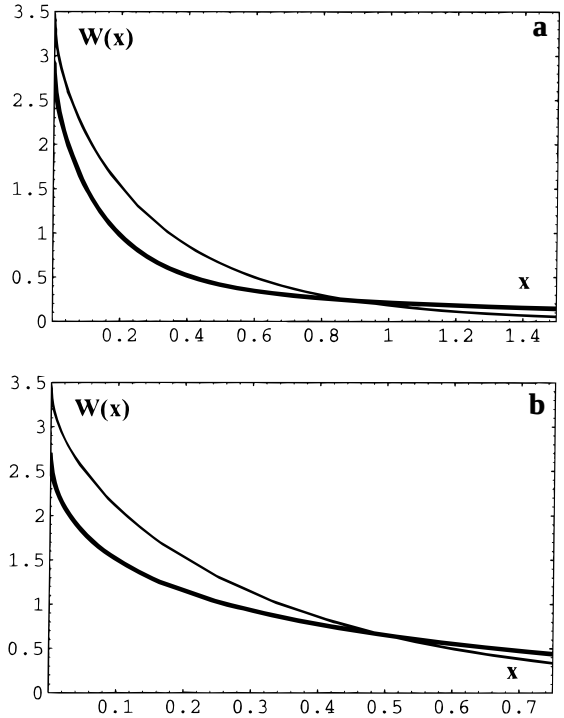

Figure 2. Line shape $W_\lambda(x)$ against reduced frequency x for various uniaxial extensions λ. The lines are symmetrical about $x = 0$, are only shown for $x > 0$, and are normalized to a weight 2. (a) $\lambda = 1$ (light) and $\lambda = 2$ (heavy line); note the shift of intensity to higher x when stretched due to the ordering ($Q > 0$, prolate ordering). (b) $\lambda = 1$ (light) and compression $\lambda = 0.5$ (heavy line); the uniaxially compressed sample is also ordered ($Q < 0$, oblate), and hence the line broadens with intensity being shifted to higher x.

lines of lesser λ as x increases, for $\lambda > 1$ (extension), and vice versa for $\lambda < 1$ (uniaxial compression). We plot $W_\lambda(x)$ against x for various λ in Figure 2. Note both positive and negative deviations away from isotropy yield broadenings. There is a sharp cusp at $x = 0$.

C. Second Moment of the Line. New methods have been recently developed to accurately measure the second moment M_2 of the NMR line for systems such as polymers.[8] Nuclear spins are sensitive to the magnitude of the dipolar or quadrupolar interaction in various ways. For example, random fluctuations in the interactions associated with thermal motion will cause spin relaxation at a rate determined by this strength. In this paper, however, we shall be concerned with coherent evolution of the spin phases under the influence of the interactions, such as might be manifest in the spectrum of frequencies associated with free precession. In cases where spins experience unique local interaction magnitudes, a distinctive frequency spectrum will arise whose structure relates directly to the orientational distribution associated with the internuclear vectors, in the case of dipolar interactions, or with the principal axis of the electric field gradient, in the case of quadrupole interactions. This interaction strength can then be determined by measuring the frequency separation of some characteristic spectral features.

In many situations of practical interest, where the spin couplings are inhomogeneously distributed, there exist no clear cut spectral features and a parameter is required which reflects the appropriate spin average. Because the dipolar and quadrupole interactions are bilinear in the spin operators, the spin precession has a phase distribution which is described by an expansion

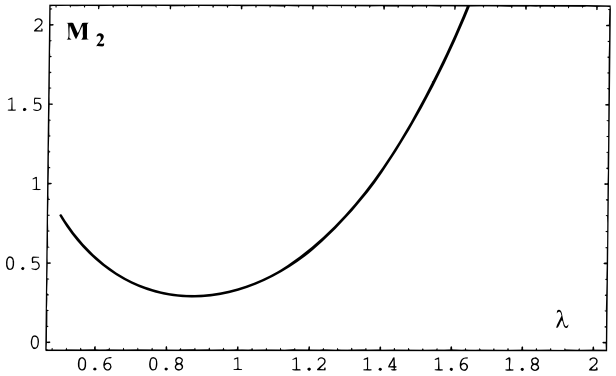

Figure 3. Second moment $M_2(\lambda)$ of the line $W_\lambda(x)$ against uniaxial extension λ. The second moment is minimal close to $\lambda = 1$ (at 0.88) and grows with anisotropy induced by extension or compression.

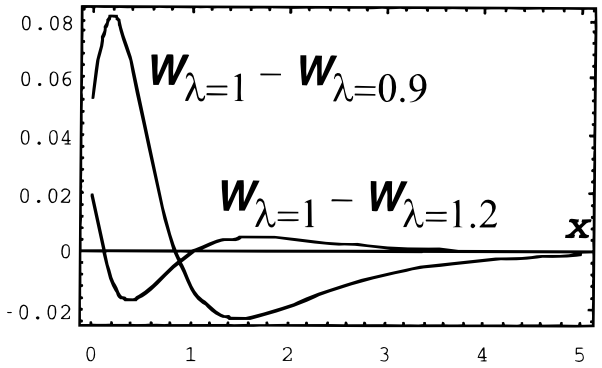

Figure 4. Differences $W_{\lambda=1}(x) - W_\lambda(x)$ in line shape plotted against reduced frequency x to reveal subtle crossings in the region $\lambda = 0.9$. The $\lambda = 0.9$ case reveals more intensity at larger x than the $\lambda = 1.2$ case, giving it a higher second moment, M_2.

of moments of even order. The predominant term is the second moment, M_2, a parameter which dominates the Bloch decay[9] in a simple one-pulse experiment, the coherence transfer in Jeener−Broekaert echoes,[10] and the time dependence of the signal amplitude in dipolar (or quadrupolar) correlation experiments.[8,11−13]

The second moment of the line, $\int_{-\infty}^{\infty} dx\, x^2 W_\lambda(x)$, is straightforward to calculate by returning to eq 8 and performing $\int_{-\infty}^{\infty} dx\, x^2$ before the averages over z and y. The δ functions render this trivially to $2\langle z^4\rangle_z\langle(1/2\lambda - [\lambda^2 + 1/2\lambda]y^2)^2\rangle_y$, the factor of 2 coming from $\Sigma_\pm$. $\langle z^4\rangle_z$ yields $^5/_3$, and $\int dy$ is elementary. Gathering terms, we find an exact expression for the second moment:

$$M_2 = \frac{1}{3}\left[\lambda^4 - \frac{2}{3}\lambda + \frac{2}{3}\frac{1}{\lambda^2}\right] \qquad (10)$$

which is plotted in Figure 3.

Although $W_\lambda(x{=}0)$ is maximal at $\lambda = 1$, that is, the intensity is shifted outward for both extensions and compressions (see Figure 2), the second moment is minimal for $\lambda = (2/3)^{1/3} \sim 0.88$ and not $\lambda = 1$. Inspection of the line shapes $W_\lambda(x)$ in the region $\lambda = 0.9-1.0$ shows a subtle crossing and recrossing of the $W_\lambda(x)$ and $W_{\lambda=1}(x)$ functions. They are very close to each other for all reduced frequencies x in this region of λ. The crossings are only revealed by plotting the differences $W_{\lambda=1}(x) - W_\lambda(x)$ against x with a greatly expanded scale (see Figure 4). Outside the region close to $\lambda = 0.9$, the curves $W_\lambda(x)$ and $W_{\lambda=1}(x)$ indeed cross as illustrated in Figure 2.

If one considers the affine deformation of angle θ and mean square dimension R^2 of a strand as λ deviates from 1, one can see that θ increases for $\lambda > 1$ and diminishes for $\lambda < 1$. R^2 increases for strands with $\theta < 54°$ and decreases for strands with $\theta > 54°$ as λ increases, and vice versa for $\lambda < 1$ (with reversals of this trend for some angles at large deviations from $\lambda = 1$). Since the splitting depends on $R^2P_2(\cos\theta)$ and is of opposite sign for $\theta < 54°$ and $\theta > 54°$, then for some strands ($\theta < 54°$ initially) the numerical value of the splitting increases with $\lambda > 1$ and decreases (for $\theta > 54°$ initially), and vice versa for $\lambda < 1$. The complicated interplay of changes of angle and mean-square dimension according to initial strand orientation means that the minimal second moment is not simply at, e.g., $\lambda = 1$ but must be located by detailed analysis. It would be interesting to know at what value of λ the second moment is minimal in real systems.

The asymptotic behavior $M_2 \sim \lambda^4$ is to be expected from this model. Individual lines are split by $\Delta\omega \sim \lambda^2 P_2$ and hence individually contribute to M_2 as λ^4. The fact that real chains have an M_2 that scales less severely than λ^4 is perhaps a surprise. One might expect that finite extensibility, topological contraints such as entanglements, and other such mechanisms by which strain might more directly influence alignment would all act to make the increase in splitting *more* effective than in a Gaussian as λ is increased. It is possible that junction fluctuations or, in the case of proton NMR, intermonomer proton−proton interactions[8] are responsible for this deviation.

IV. Conclusions

Brereton's counterintuitive result, that even stretched Gaussian networks should have no NMR splitting, is correct. We present a slightly different analysis and get the same result but with a corrected analytical form. Plots of the corrected result have a more physical appearance. We have given an exact analytic expression for the second moment M_2 of the NMR lines of Gaussian networks in order to confront newly available accurate measurements. To reproduce the actual splittings observed when networks are stretched, one needs new ingredients, either incipient nematic interactions, ordinary steric interactions,[1] anisotropic junction point fluctuations,[14] or more involved effects such as complex formation histories with compositional fluctuations and/or rigid-rod cross-links.

Acknowledgment. We are indebted to M.G. Brereton for discussions and correction of an error in an early stage of this work. E.T.S. and P.T.C. acknowledge support from the National Science Foundation (DMR-9412701) and the New Zealand Foundation for Research, Science and Technology, respectively.

Appendix A. Orientational Potential and Order of a Bond of a Network Chain

The probability of a link j having position $\mathbf{x}_j$ and orientation $\mathbf{u}_j$ is

$$p(\mathbf{u}_j,\mathbf{x}_j) \sim \exp\left[-\frac{3}{2b^2}\left(\frac{\left(\mathbf{x}_j - \frac{b}{2}\mathbf{u}_j\right)^2}{j-1} + \frac{\left(\mathbf{R} - \mathbf{x}_j - \frac{b}{2}\mathbf{u}_j\right)^2}{N-j}\right)\right] \tag{A1}$$

that is, the weight associated with a random walk of $j - 1$ steps from **O** to one end of the rod at $\mathbf{x}_j - (b/2)\mathbf{u}_j$ and a walk of $N - j$ steps from the other end at $\mathbf{x}_j + (b/2)\mathbf{u}_j$ to **R**. The orientational distribution $p(\mathbf{u}_j)$ regardless of the position of the link then derives from $p(\mathbf{u}_j) = \int d\mathbf{x}_j\, p(\mathbf{u}_j,\mathbf{x}_j)$. This integration can be performed by collecting terms in x^2 and x and then completing the square in the exponent. There remains terms in $\mathbf{R}\cdot\mathbf{u}_j$ which are important and terms independent which we ignore. The result is, on gathering all such terms in the exponent:

$$p(\mathbf{u}\cdot\mathbf{R}) \sim \exp\left[-\frac{3R}{(N-1)b}\hat{\mathbf{R}}\cdot\mathbf{u}\right] \tag{A2}$$

where we have dropped the label j on the link vector since the result is the same for all links on the strand.

The constraint to a cone with axis $\hat{\mathbf{R}}$ is weak since the rotations of the short bond $b\mathbf{u}_j$ cause little bias of the chains of jointed rods attached at each end, that is, little stretch of the "entropic springs" attaching the ends of the bond to the cross-links. We write the potential in the form $p(\mu) \sim \exp(a\mu)$ where $\mu = \cos\theta = \mathbf{u}_j\cdot\hat{\mathbf{R}}$ defines the angle of the bond with **R** and the polar axis and where $a = [3/(N-1)](R/b)$. In this frame the order parameter is $Q(R) = \langle {}^3/_2\mu^2 - {}^1/_2\rangle$ which can be trivially evaluated using the distribution function $p(\mu)$:

$$Q(R) = a^2/15 + \ldots \tag{A3}$$

and thus we obtain the result eq 1 for $Q(R)$. Reference 7 also starts with freely jointed rods and using the classic Rayleigh method of random flights reduces the problem to that of extensible Gaussian subunits. The result for $Q(R)$ is essentially that produced here.

References and Notes

(1) Brereton, M. G. *Macromolecules* **1993**, *26*, 1152.
(2) Kupfer, J.; Finkelmann, H. *Makromol. Chem. Phys. Commun.* **1994**, *195*, 1353.
(3) Kundler, I.; Finkelmann, H. *Macromol. Rapid Commun.* **1995**, *16*, 679.
(4) Disch, S.; Schmidt, C.; Finkelmann, H. *Makromol. Rapid Commun.* **1994**, *15*, 303.
(5) Remmers, H.; Finkelmann, H. Ph.D. thesis, unpublished.
(6) Verwey, G. C.; Warner, M. *Macromolecules*, in press.
(7) Cohen-Addad, J.-P.; *J. Phys. Fr.* **1982**, *43*, 1509.
(8) Callaghan, P. T.; Samulski, E. T. *Macromolecules* **1997**, *30*, 113.
(9) Abragam, A. *The Principles of Nuclear Magnetism*; Oxford University Press: Oxford, U.K., 1961.
(10) Jeener, J.; Broekaert, P. *Phys. Rev.* **1967**, *157*, 232.
(11) Cohen Addad, J.-P. *J. Chem. Phys.* **1975**, *63*, 4880 and references therein.
(12) Collignon, J.; Sillescu, H.; Spiess, H. W. *Colloid Polym. Sci.* **1981**, *259*, 220.
(13) Kimmich, R.; Fischer, E.; Callaghan, P. T.; Fatkullin, N. *J. Magn. Reson.* **1995**, *A117*, 53.
(14) Brereton, M. G. *Macromolecules* **1991**, *24*, 6160.

MA9618033